On estimating Gross Primary Productivity of Mediterranean grasslands under different fertilization regimes using vegetation indices and hyperspectral reflectance

Sofia Cerasoli[1], Manuel Campagnolo[1], Joana Faria[1], Carla Nogueira[1], Maria da Conceição Caldeira[1]

[1]CEF, Centro de Estudos Florestais, Instituto Superior de Agronomia, Universidade de Lisboa, PT.

Correspondence to: Sofia Cerasoli (sofiac@isa.ulisboa.pt)

Key-words: hyperspectral reflectance, remote sensing, carbon sequestration, pasture

Running-title: GPP estimates in grasslands by optical sensors

Abstract: We applied an empirical modelling approach for Gross Primary Productivity (GPP) estimation from hyperspectral reflectance of Mediterranean grasslands undergoing different fertilization treatments. The objective of the study was to identify combinations of vegetation indices and bands that better represent GPP changes between the annual-peak of growth and senescence dry out in Mediterranean grasslands.

In-situ hyperspectral measurements of vegetation were collected at the same time as CO_2 gas exchange measurements were performed in control (C) and fertilized plots with added nitrogen (N), phosphorus (P) or the combination of N, P and potassium (NPK). Reflectance values were aggregated, according to their similarity (r>90%), in 26 continuous wavelength intervals (Hyp). Also, the same reflectance values were resampled reproducing the spectral bands of both Sentinel-2A Multispectral Instrument (S2) and Landsat 8 Operation Land Imager (L8) simulating the signal that would be captured in ideal conditions by either Sentinel-2A or Landsat 8.

The LEAPS procedure was applied to select the best set of the vegetation indices or spectral bands for GPP estimation using Hyp, S2 or L8. The LEAPS selected some vegetation indices putting in evidence their explanatory power as indicators of the dynamic changes occurring in community vegetation properties such as canopy water content (NDWI) or chlorophyll and carotenoids/chlorophyll ratio (MTCI, PSRI, GNDVI) and underlining their importance for grasslands GPP estimates.

For Hyp and S2, bands showed similar explanatory power than vegetation indices to estimate GPP. A two-step LEAPS procedure allowed us also to identify spectral bands with potential for improving GPP estimates. This procedure clearly indicates the shortwave infrared region of the spectra as promising for this purpose. The comparison of S2 and L8 based models showed similar explanatory power of the two simulated satellite sensors when spectral bands were adopted.

Altogether our results show the potential of sensors on board of Sentinel 2 and Landsat 8 satellites for monitoring grasslands phenology and improving GPP estimates in support of a sustainable agriculture management.

1. Introduction:

Mediterranean grasslands are high biodiverse ecosystems, covering around 22% of the European Union land area, and providing important ecosystem services such as forage production (Bugalho and Abreu, 2008; Díaz-Villa et al., 2003). These ecosystems are subjected to large pressures under global change (Sala, 2000), namely by the increasing availability of nutrients (e.g., phosphorus (P) and nitrogen (N)) due to human use of fertilizers, and N deposition (Ceulemans et al., 2014; Galloway et al., 2004; Peñuelas et al., 2013) and by a decrease and shift in seasonal patterns of precipitation (Costa et al., 2012; Kovats et al., 2014). The contemporary changes in water and nutrients supply can affect species composition, biomass, phenology along the life cycle of annual grasslands (Harpole et al., 2007), compromising their productivity. In particular, the onset and extension of the senescence period, largely dependent on soil water availability, can be affected in Mediterranean grasslands with great impacts in their functioning (Aires et al., 2008a, 2008b; Jongen et al., 2013; Xu and Baldocchi, 2004).

Using remote sensing based information to evaluate GPP brings important advantages both from a scientific and management point of view. Spectral retrievals collected from optical sensors on board of remote platforms may provide information on many biophysical properties of vegetation and can be usefully employed for monitoring and modelling ecosystems GPP in a cost and time-effective way (Schimel et al., 2015). Also, for land managers, the capability of making timely grassland management decisions may improve the use and sustainability of these ecosystems.

GPP estimation models integrating remote sensed observations increased considerably in the last decades (Beer et al., 2010; Grimm et al., 2008). Such models are generally based on the Light Use-Efficiency (LUE) concept (Monteith, 1972, 1977), which defines GPP as a function of the fraction of radiation absorbed by vegetation (fPAR), which in turn depends on green leaf area and the efficiency by which light energy is used to fix carbon during photosynthesis (i.e. LUE) (Cheng et al., 2014; Yuan et al., 2014).

Based on this approach large efforts have been put to derive vegetation indices able to represent the green leaf area and LUE. The NDVI is widely used for its known linear relationship with fPAR (Fensholt et al., 2004; Joel et al., 1997; Myneni and Williams, 1994). However, some exceptions are reported in the literature. For example in highly productive environments, such as grasslands, NDVI becomes easily saturated, not responding to increased leaf area and LUE, and the regression observed is no more linear (Vescovo et al., 2012; Viña and Gitelson, 2005).

In annual grasslands, such as the Mediterranean, control on ecosystem carbon balance is generally considered related mainly to the amount of green leaf area, while little LUE changes are expected (Gamon, 2015). Nonetheless, several studies reported a hysteresis in LUE in grasslands when the duration of the study encompasses the whole life cycle (Nestola et al., 2016; Perez-Priego et al., 2015).

The Photochemical Reflectance Index (PRI) is frequently adopted as a proxy of LUE (Gamon et al., 1997; Peñuelas et al., 1995). PRI in the short term mirrors the dynamic of the xanthophylls cycle (Peñuelas et al., 1995) which is related to thylakoid energization and hence to light harvesting by photosynthesis. In the long term was found to be correlated with the ratio of carotenoids to chlorophyll (Filella et al., 2004; Porcar-Castell et al., 2012) and hence to plant senescence, since

chlorophyll degradation and N export is a distinctive process of leaf ageing (Thomas, 2013). However, also PRI shows some drawbacks, since it is largely affected by species identity, leaf age or environmental conditions (Peñuelas et al., 1995) and by sensors geometry and atmospheric factors (Moreno et al., 2012). Hence the performance of models integrating PRI is frequently below the expected (Perez-Priego, 2015).

5 As a result, other vegetation indices have been tested as alternatives to NDVI and PRI for GPP estimation. Rossini et al. (Rossini et al., 2012), in an subalpine grassland obtained the best model to estimate GPP adopting together the MERIS Terrestrial Chlorophyll Index (MTCI) (Dash and Curran, 2004), a proxy of chlorophyll, and PRI. In another study, in a subalpine grassland, Sakowska (Sakowska et al., 2014), found that the red-edge NDVI, a modified NDVI, where the infrared band is substituted with a red-edge band (Gitelson and Merzlyak, 1994) improved GPP estimates. In Mediterranean

10 grasslands with different N and P fertilization level, PRI together with solar induced fluorescence improved GPP estimates (Perez-Priego et al., 2015). In a semi-arid grassland Vicca et al. (Vicca et al., 2016) observed that several vegetation indices including NDVI and the Normalized Different water Index (NDWI) (Gao, 1996), a proxy of vegetation water content, were able to capture the drought effect on GPP.

Altogether these results clearly indicate the need for further studies aiming to identify the vegetation indices and the regions

15 of the spectra of potential interest for GPP estimates of grasslands under different environmental constraints, such as nutrients availability.

The adoption of a specific model and vegetation index depends also frequently on the availability of remote sensed products at a suitable spatial and temporal scale. In the case of local scale monitoring of managed grasslands, sensors with high spatial resolution will produce better results than sensors with coarse spatial resolution. In this study we opted for using data from

20 Sentinel-2A MSI (Multi-Spectral Instrument), (hereafter named S2) and Landsat8 OLI (Operational Land Imager) (hereafter named L8), for their spatial resolution, (10-20m for S2 and 30m for L8) more suitable for representing grasslands spatial heterogeneity and hence better adapted to implement management options from a precision agriculture perspective. The L8 provides reflectance in 7 bands ranging from the visible to the short wave infrared region (SWIR) (Loveland and Irons, 2016), but its main drawback is the long revisiting time of 16 days. The recently launched S2 covers the regions of the

25 visible and near-infrared and the SWIR in 13 bands with at least five days revisiting time when both S-2A and S-2B platforms will become operational (Drusch et al., 2012).

Field collection of vegetation reflectance by hyperspectral sensors is less cost-effective and more time consuming than satellite remote sensed data but presents the advantage of providing reflectance in numerous, high resolution, wavelengths (Porcar-Castell et al., 2015). Therefore, it can be usefully employed for identifying which wavelengths best mirror

30 biophysical properties and physiological status of vegetation (Balzarolo et al., 2015; Matthes et al., 2015) and put in evidence regions of the spectra of potential interest for GPP modelling actually not exploited by remote sensors. The high detail of spectral resolution (1 nm nominal) is a further advantage of hyperspectral measurements. In particular, it allows comparing the performance of similar vegetation indices available from different satellite platforms resampling hyperspectral information to match spectral bands of different remote sensors.

The aim of this study was to identify combinations of vegetation indices and bands that better represent GPP changes in the period comprised between the annual-peak of growth and senescence dry out in Mediterranean grasslands subjected to different fertilization treatments.

To achieve this goal, in situ hyperspectral measurements of vegetation reflectance were employed to estimate GPP in

5 Mediterranean grasslands before and after the annual peak of growth was achieved. A set of vegetation indices proposed in the literature were calculated and the performance of models to estimate GPP based on linear combinations of vegetation indices and bands were compared.

Whenever possible, vegetation indices were also calculated simulating S2 and L8 bands and the performance of GPP estimates based on remote platforms and in situ hyperspectral measurements compared.

10 The specific objectives of the study were: (i) Identify a set of vegetation indices useful to optimize a GPP model for Mediterranean grasslands ; (ii) Compare the performance of GPP models employing vegetation indices only and in combination with spectral bands; (iii) Finally, compare GPP models using spectral information obtained from hyperspectral sensors with similar models obtained from S2 and L8 platforms.

2. Material and Methods

2.1 The study site

Our study was conducted in a semi-natural Mediterranean grassland at Companhia das Lezírias, an estate of approximately 15 000 ha, located north-east of Lisbon, Portugal (38°49´45.13´´N, 8°47´28.61´´W). The grassland plant community is
5   composed mainly of annual C3 species. The climate is Mediterranean, with mild, wet winters and hot, dry summers. Long-term (1961–1990) mean annual rainfall is 709 mm. Mean annual temperature is 15.9 °C (INMG, 1991). Site topography is flat and the soil is a well-drained deep Haplic Arenosol (WRB, 2006).

2.2 Experimental design

The grassland studied is part of the Nutrient Network experiment (http://www.nutnet.umn.edu; Borer et al., 2017;
10   Seabloom et al., 2013). Plots (5m x 5m) were established in 2012, in a randomized block design. Factorial combinations of nitrogen (N), phosphorus (P), and potassium plus micronutrients (K), a total of eight treatments per block, including the control (C) with no added nutrients, were considered. All nutrients were added at a rate of 10 g. N. m^{-2} yr^{-1}. N was added as slow-release urea (60-90 days), P was added as triple-super phosphate and K as potassium sulphate. Micronutrients (6% Ca, 3% Mg, 12% S, 0.1% B, 1% Cu, 17% Fe, 2.5% Mn, 0.05% Mo, and 1% Zn) were added with K only once, at the start of the
15   study to avoid possible micronutrient toxicity. In this study, only four fertilization treatments were considered: C, N, P and NPK. Each one of these treatments was repeated twice per block, a total of 24 plots were considered (2 replicates X 4 treatments X 3 blocks).

2.3 Environmental measurements

Temperature, PAR and relative humidity were measured in situ using a VP-3 humidity temperature and vapour pressure
20   sensor and QSO-S PAR Photon Flux sensor (Decagon Devices, Pullman, USA) logged every 30 min (EM50 data logger, Decagon Devices, Pullman, USA). Precipitation was recorded using a tipping bucket rain gauge (RG2, Delta-T Devices, Cambridge, UK). Soil water content (SWC) was continuously measured, at a depth of 10 cm, using EC-5 soil moisture sensors (Decagon Devices, Pullman, USA). The rain gauge and soil sensors were connected to a CR1000 and AM16/32B multiplexer data logger (Campbell Scientific, Logan, USA).

25   ### 2.4 Field Measurements

2.4.1 NEE and R from a closed system IRGA

Grassland net ecosystem exchange (NEE) was measured with a closed chamber (40 cm X 40 cm X 54 cm) of polymethylmethacrylate (3 mm thick) inserted into a permanent frame buried 5 cm into the soil. Radiation transmittance was higher than 95%. The same chamber was covered with a reflective cloth for dark respiration (R) measurements. Air

temperature inside the chamber was continuously monitored and PAR was measured at beginning and end of measurements with a ceptometer (AccuPAR-LP80, Decagon Devices, Inc. Pullman, WA, USA). Fans in the chamber ensured air circulation. The chamber was connected to an infrared gas analyser (LI-840, Li-Cor, Lincoln, NE, USA) measuring CO_2 and water vapour. Each measurement was no longer than 3 min. Fluxes were calculated based on the rate of change of CO_2

5 inside the chamber, after an initial period of at least 10 seconds. Flux calculations and corrections for CO_2 water vapour dilution followed Perez-Priego (2015). GPP was obtained by detracting R from NEE at each measurement. All plots were measured between 11:00 and 13:00 on clear sky sunny days. Measurements were performed during the 2016 growing season. Two field campaigns were carried out during vegetation growth, day 1 (31st March to 1st April) and day 2 (24th to 25th April) and two during the senescence phase, day 3 (19th – 20th May) and day 4 (1st-3rd June).

10 **2.4.2 Leaf area and biomass**

The Plant Area Index (PAI) was indirectly measured with a linear PAR ceptometer (AccuPAR LP-80 Decagon Devices Inc., Pullman, WA, USA). The ceptometer measures the fraction of PAR intercepted by the canopy (fPAR) according to equation (1):

$$fPAR = \frac{1 - PAR_t}{PAR_i} \tag{1}$$

15 The fPAR was considered approximately equal to absorbed radiation, as the amount of reflected radiation in the PAR range is usually low (Gower et al., 1999). For each plot, 6-8 measurements above (PAR_i) and below (PAR_t) the canopy were taken and averaged.

The PAI is calculated by inversion of the Beer-Lambert law (equation 2):

$$fPAR = 1 - e^{-K*PAI} \tag{2}$$

20 where K is the light extinction coefficient, which depends on the leaf angle distribution of the canopy, in this study considered spherical distributed, and on the zenith angle of the probe, calculated by the ceptometer with basis on the geographic coordinates of the local and date and time of measurements. To avoid low solar zenith angles all measurements were performed around solar noon. As the growing season progressed some species started to senesce. In order to estimate the fraction of PAR absorbed only by photosynthesizing components of the canopy ("green" PAI, PAIgr), PAI was

25 multiplied by a normalized (by scaling between 0 and 1) greenness index (GI, calculated as a ratio between the digital number values of green and the sum of red, green, and blue digital number values) derived from the analysis of digital pictures of the plots taken at each measurements day around solar noon (Cyber-shot DSC-W530, SONY), using the Phenopix R package (Filippa et al., 2016).

A strip of vegetation (0.1 mx1 m) within each plot was also collected close to the peak growth and biomass divided into

30 functional types (legumes, forbs, graminoids) and dried in an oven.

2.4.3 Hyperspectral measurements of vegetation reflectance

At each field campaign, hyperspectral observations of all plots were also acquired with a FieldSpec3 spectroradiometer (ASD Inc., Boulder, USA), which provides reflectance of vegetation in the range of 350-2300 nm. The spectral resolution (Full-Width-Half-Maximum) is 3 nm at 700 nm and 10 nm at 1400 nm and 2100 nm. The sampling interval is 1.4 nm for the spectral region of 350-1000 nm (visible and near infrared) and 2 nm for the spectral region of 1000-2500 nm (short-wave infrared). Spectra at 1nm intervals are obtained from a cubic spline interpolation function. Five spectra were collected for each plot, each representing the average of 25 spectra, employing a bare fibre optic cable (with an instantaneous field of view of 25°) inserted into a pistol grip at approximately 90 cm above the canopy. A white reference of known reflectance (Spectralon panel, Labsphere, Inc., North Sutton, USA) was used to normalize for variations in atmospheric conditions and to convert the measurements into absolute reflectance (Ref.). All measurements were conducted immediately after grassland gas exchange measurements, within two hours around solar noon, to minimize the effects of shadowing and solar zenith changes.

2.5 Data analysis

All statistical analyses were performed using open-source R (R Core Team, 2016). We used the lme4 package (Bates et al., 2014) to perform linear mixed effect analyses of the effect of the fertilization and control treatments on NEE, R, GPP and PAIgr. Treatment and date were the fixed effects and the block was the random effect. Conditions of homoscedasticity and normality were always verified by visual inspection for residuals. P-values were obtained by likelihood ratio tests of the full model with the effect in question against the model without the effect in question. A Tukey test was used for post-hoc comparison using the multcomp package (Hothorn et al., 2008).

The full spectra of vegetation reflectance retrieved from the Fieldspec was used to model GPP, after excluding noisy values in the range 1350-1400 nm and 1800-1950 nm. Our P=1748 original explanatory variables are $x_{350},...,x_{2299}$ where x_λ represents the reflectance in the narrow band $[\lambda, \lambda+1]$ (nm) and our response variable is the GPP (μmol m^{-2} s^{-1}). A total number of 96 observations were available (4 treatments X 2 replicates X 3 blocks X 4 dates). Since we have 1748 explanatory variables and just 96 observations, hence a high level of redundancy in our data, the dimensionality was reduced by grouping variables that belong to intervals of wavelengths where all variables are highly correlated. A hierarchical cluster analysis was performed to reduce the number of predictors from P=1748 to P=25 groups of contiguous variables named Bands. The distance between two variables is the correlation coefficient and the distances within a band is given by the complete link criterion to guarantee that $r(x_{\lambda a}, x_{\lambda b}) > 0.90$ for any pair of variables $(x_{\lambda a}, x_{\lambda b})$ within each group.

Formally, wherever all pairs of variables $x_{\lambda a}$ and $x_{\lambda b}$ -- such that $\lambda_1 \leq \lambda_a < \lambda_b \leq \lambda_2$ – are highly correlated, i.e. $r(x_{\lambda a}, x_{\lambda b}) > 0.9$, then the original variables $x_{\lambda 1},...,x_{\lambda 2}$ in the interval $[\lambda_1, \lambda_2]$ are replaced by a new variable $x_{[\lambda_1, \lambda_2]}$, which is the arithmetic mean of $x_{\lambda 1},...,x_{\lambda 2}$.

Reflectance values were also resampled to simulate bands of Sentinel-2A MSI (S2) and Landsat8 OLI (L8). For each sensor and band $[\lambda_1, \lambda_2]$, we calculated the response as a weighted mean of $x_{\lambda 1},...,x_{\lambda 2}$, where the weights are the coefficients of the spectral response function (Barsi et al., 2014; ESA, 2018). The list of S2 and L8 bands used in this study is shown in table 1. Vegetation indices (VIs) (Table 2) were calculated from hyperspectral (Hyp), or simulated S2 and L8 sensors (Table 1). The

5 VIs were selected from the literature with basis based on their relation to biophysical properties of vegetation affecting GPP. The NDVI and the NDVIre, are considered a proxy of fPAR; the Green Normal Difference Vegetation Index (GNDVI) , the MERIS Terrestrial Chlorophyll Index (MTCI) and the chlorophyll index (CI) are representative of chlorophyll-a and N content, while the Photochemical Reflectance Index (PRI) and the Plant Senescence Reflectance Index (PSRI) are expected to mirror changes in the ratio of carotenoids to chlorophyll. Finally, the Normalized Difference Water Index (WBI) and the

10 Normalized Difference Water Index (NDWI) are considered proxy of tissue water content.

A multiple linear regression (MLR) was adopted to model the relation between our explanatory variables (bands and VIs) and the response variable (GPP). Since the number of observations is only roughly twice as large as the number of new explanatory variables we performed a variable selection and excluded variables that do not contribute significantly to the goodness-of-fit of our model. Although the dimensionality of the problem is very large, it can be solved efficiently by the

15 LEAPS algorithm (Furnival and Wilson, 1974) available through the R package leaps (Lumley, 2009).

A nested approach was adopted to formally test which model better explained GPP. A preliminary test showed that better results were obtained with exponential regressions and therefore lnGPP was adopted as the response variable in all analyses. The general model was $\ln GPP \sim \sum_{j,1}^{n} vj$, where v are vegetation indices (VIs) or optical bands (B) from Hyp grouping procedure or from simulated S2 or L8 data. The subset of v_j was selected by maximizing the adjusted R^2 among all possible

20 combination of predictors.

The LEAPS procedure returns and optimal model named L. However, L may include variables which contribute only marginally for the overall adjusted R^2. To further reduce the dimensionality of the predictors, we test sub-models of L (obtained by backwards stepwise selection of predictors) against the LEAPS optimal model L. When sub-models of L were found not to be significantly worse than L, at a significance level alpha=0.05, then we considered the most parsimonious of

25 those sub-models as the optimal solution. A F-test was used to perform those comparisons. The analysis was repeated separately for all vegetation indices (VIs) and bands (B) from Hyp, S2 or L8 data, obtaining an optimal model for each sensor.

Besides determining the adjusted R^2 for the optimal model from the full sample, we applied a bootstrap procedure (N=10000 iterations) to estimate the distribution of the adjusted R^2 in the whole population (Ohtani, 2000). This allowed us to estimate

30 quantiles (25%-75%) for adjusted R^2 and also compare the adjusted R^2 distributions among models. In particular, it permits to estimate the probability that some model A has a higher adjusted R^2 than an alternative model B.

Two-sstep models were also used to investigate if optical bands had the potential to improve models based only on vegetation indices (VIs). Toward that end, bands (B) were added to the optimal models obtained by the procedure above described denoted by Hyp-VIs, S2-VIs and L8-VIs (step 1). Using step 1 as the base model, we applied LEAPS to determine

the subset of bands that maximized the overall adjusted R^2. As before, we applied a F-test (alpha=0.05) to possibly reduce the number of bands in the optimal model. As a result, we defined the optimal two-sstep models: Hyp-VIs+B, S2-VIs+B and L8-VIs+B. Finally, for Hyp, S2 and L8, we performed a F-test to compare the one step optimal model with the correspondent two-ssteps optimal model. A low p-value for this F-test indicates that the two-step model is significantly better and means that bands, in addition to vegetation indices, contribute for an improved modelling of GPP.

3. Results

3.1 Conditions during the experimental period

During the period of measurements, from March 31 to June 3, the average daily PAR and temperature increased progressively, ranging from 630 $\mu molm^{-2}s^{-1}$ to 1000 $\mu molm^{-2}s^{-1}$ and from 9.6 ˚C to 17˚C, respectively (Fig.1a). Soil water content (SWC) (Fig. 1 b) showed fluctuations according to rainfall events, ranging from 0.05 to 0.2 m^3m^{-3}. During the experimental period, rainfall was concentrated in the first half of April and at the beginning of May. Along the experimental period rainfall recorded was 195mm, corresponding to the 33% of the whole year.

3.2 The effect of fertilization on leaf area and species composition

From the beginning to the end of the study period, PAI increased on average 4 fold from 1 to 4 (Fig2a). In all treatments, the increase in PAI was completed by May 20 and no further increase was observed in the last measurement (June 3). On the contrary, at the beginning of the experiment PAIgr (Fig2b) showed an increasing tendency similar to PAI but from May 20 onwards, the trend changed and a decreasing trend was then observed corresponding to the onset of grassland senescence.

The fertilization treatments influenced both the PAI (P<0.000) and the PAIgr (Fig2b, PAIgr) (P<0.000) being both significantly higher for treatments NPK and P than for treatment C (P<0.001). No differences were observed between C and N treatments (P>0.05). In both PAI and PAIgr the treatment P showed similar values to NPK, with the exception of the first measurements day (April 1). The grassland communities fertilized with NPK had a higher and earlier leaf area growth when compared to the other treatments.

The fertilization treatments also influenced the functional composition of grasslands (Table 3). In the NPK treatment the percentage of graminoids was higher than in any of the other treatments. P treatment showed a higher percentage of legumes and in the C and N treatments forbs were the dominant functional group.

3.3 The effect of fertilization on GPP

The ability of grasslands to sequester atmospheric carbon dioxide was not affected by fertilization treatments. The NEE (Fig.3a) and the GPP (Fig.3c) did not reveal any statistical significant difference among treatments (P>0.05). On the contrary, the rate of respiration (Fig.3b, R) was affected by the fertilization treatment (P<0.05), being on average higher for treatments NPK and P than C. CO_2 gas exchanges were influenced by the grassland life cycle and marked trends were

observed along the measurement period. NEE showed an average drop of 74%, shifting from -14.47 $\mu molm^{-2}s^{-1}$ to -3.67 $\mu molm^{-2}s^{-1}$, from April 01 (day 1) to June 03 (day 4) (P<0.000). This decrease in NEE rate was particularly evident from the second to the third measurement day, after the annual peak of grassland growth was achieved (Fig. 3a). R also showed differences along the experimental period (P<0.000) but the trend observed was different. R increased from the first to the

5   second measurement day, from 8.22 $\mu molm^{-2}s^{-1}$ to 13.65 $\mu molm^{-2}s^{-1}$ and then decreased toward the end of the experiment (Fig. 3b). GPP also changed significantly along the studied period (P<0.000), decreasing from 25.72 $\mu molm^{-2}s^{-1}$ on April 25 (day 2) to 12.12 $\mu molm^{-2}s^{-1}$ on June 3(day 4).

3.4 Vegetation reflectance

The reflectance of vegetation (Ref) varied on average between 0 and 0.4 (Figure 4a).The Cluster analysis created 25 bands

10   (Fig. 4b) based on Ref similarity of contiguous wavelengths (r>90%). Bands were narrower in the visible region (350 nm to 750 nm) than in the NIR (750 nm to 1350 nm) and in the SWIR (1350 nm to 2300 nm) region. In particular, in the red-edge region, between 698 and 732nm 6 different bands were identified, corresponding to a steep increase in reflectance observed in this region of the spectra.

3.5 Vegetation indices

15   Adopting wave bands obtained by cluster analysis (Fig.4b) several vegetation indices were calculated (Table 2). The average values of the indices GNDVI, NDWI, PSRI and MTCI are shown in figure 5. Other indices are omitted from the figure for showing very similar trends to the ones represented (NDVI, NDVIre, WBI, CI) or not being significantly correlated with the response variable (PRI). All of them showed larger changes during the study period, particularly after April 25 (day 2), when the annual peak of growth was achieved.

20   The GNDVI (Fig. 5a) showed small changes among treatments and dates, with a significant drop of 20% observed from April 1 to June 3 (P<0.000), and significant differences in the NPK and P treatments (P<0.001) as compared to C but differences were not evident anymore on June 3 (day 4). The MTCI (Fig.5b) showed a large drop particularly evident after April 25 (day 2). At April 1 (day 1), the effect of fertilization was evident in treatments NPK and P as compared to C (P<0.001), however along the experimental period differences among treatments diminished and by June 3 (day 4) no

25   differences among treatments were observed. The NDWI (Fig.5c) showed a similar temporal trend with a marked decrease from April 1 to June 3 (P<0.001). Also for MTCI, the NPK and P treatments showed always higher values than C (P<0.001), suggesting a positive impact of the higher nutrient availability on tissue water content. The PSRI had an opposite trend, showing on average threefold increase from April 1 to June 3 (P<0.000) and a tendency to lower values in fertilized treatments as compared to C (P<0.001) for NPK and P and P<0.01 for N).

Significant regressions were established between GPP and all the vegetation indices considered (Table 4) with the exception of PRI. The NDWI was the index that explained the higher proportion of variability of GPP, which is the result of the progressive drying out of vegetation toward the end of the growing season.

3.6 GPP estimates by multiple linear regression models

5   The LEAPS procedure selected VIs or Bands as predictor variables retrieved from Hyperspectral data (Hyp) or simulating Sentinel-2 MSI (S2) and Landsat8 OLI (L8) sensors.

Models adopting only VIs as predictor variables (Hyp-VIs and S2-VIs) performed similarly with a considerable overlap of adjusted R^2 (Table 5). On the contrary, the L8-VIs model showed a lower performance (lower adjusted R^2) than Hyp-VIs and S2-VIs models (Table 5). Bootstrap results allowed us to conclude, at a confidence level of 90%, that Hyp-VIs has higher

10   adjusted R^2 than L8-VIs.

The selection of VIs in the Hyp-VIs and S2-VIs models exhibited a similar spectral pattern. Both models included PSRI and GNDVI. On the contrary, NDVI, the most frequently adopted index as green leaf area proxy was not included in the Hyp-VIs model but only in the S2-VIs. Two of the indices included in the Hyp model are related with water balance (WBI) and water tissue content (NDWI). The S2 model includes also MTCI, which represents chlorophyll-a and N.

15   Models including only bands (-B) showed similar performance to respective models employing vegetation indices (-VIs). Only in the case of L8, where just one vegetation index (NDVI) was available, bands (L8-B) led to better modelling of GPP than vegetation indices (L8-VIs)). Similar spectral patterns were also observed in the selection of bands for GPP estimate for all sensors (Hyp, S2, L8). A common pattern is the inclusion of bands in the SWIR region strongly represented in the Hyp-B ($R_{1951-2299}$, $R_{1209-1327}$, $R_{1328-1349}$), S2-B (B11) and L8-B (B6 and B7) models. The red edge region of the spectra was also

20   largely represented in the Hyp-B ($R_{724-732}$, $R_{706-710}$, $R_{702-705}$, $R_{698-701}$, $R_{716-723}$) and S2-B (B5, B6 and B7) underlining the importance of this region for vegetation reflectance.

The LEAPS two-step procedure allowed to identify bands with potential to improve the VIs based models, identifying regions of the spectra generally not adopted in vegetation indices. For both Hyp and L8 the two-step model (VIs + B) increased significantly ($P<0.010$) the performance of the model, while for S2 the difference between S2-VIs and S2-VIs+B

25   model, in spite of still significant, is less marked ($P<0.05$). The bootstrap indicated that the probability of the Hyp-VIs+B being significantly better (alpha=0.05) is 83% when compared to S2-VIs+B and 81% when compared to L8-VIs+B. On the contrary, the S2-VIs+B and the L8-Vis+B models exhibit roughly the same explanatory power. In all the VIs+B models, bands in the SWIR region were included. The second region of the spectra more represented in the Hyp-B and Hyp-VIs+B model was the red-edge.

4. Discussion

4.1 Best VIs for GPP estimation

The LEAPS procedure selected several indices as significant predictor variables for GPP in the Hyp-VIs and S2-VIs model (Tab. 5). The vegetation indices selected in the Hyp-VIs and S2-VIs models are known to represent different properties of
5 vegetation, specifically: the green fraction of the leaf area (GNDVI and NDVI) , the chlorophyll-a and N concentration (MTCI), the ratio carotenoids/chlorophyll (PSRI) and the tissue water content (NDWI,WBI). Each of these traits has a major role in GPP.

Among the vegetation indices selected in the multiple linear models, both the Hyp-VIs and the S2-VIs included the PSRI (Merzlyak et al., 1999) which is generally applied to detect the occurrence of vegetation senescence. PSRI is able to capture
10 changes in the carotenoids/chlorophyll ratio which occur during vegetation senescence since chlorophyll declines more rapidly than carotenoids (Merzlyak et al., 1999). In this study, PSRI increased in all treatments after April 25, where the maximum peak of growth (Fig.2,b) was achieved and close to the onset of canopy drying out. Another index known to be related with the carotenoids/chlorophyll ratio, the PRI (Filella et al., 2009), showed no correlation with GPP in our study. These results are in contrast with previous studies (Perez-Priego et al., 2015). However, a low performance of PRI in
15 representing the carotenoids/chlorophyll ratio has been already observed in semiarid grasslands (Vicca et al., 2016). In crops, a good agreement between PRI and pigment pools was observed at leaf (Gitelson et al., 2017a) but not at stand level. (Gitelson et al., 2017b). Differences in the last two studies were ascribed to changes in canopy structure (e.g., changes in leaf inclination angle) over the growing season.

The Hyp model also put in evidence the importance of changes in canopy water content, as both the NDWI (Gao, 1996) and
20 the WBI (Penuelas et al., 1997) were included in the model. Changes observed in NDWI along the experiment and the good correlation observed between NDWI or WBI and GPP is an evidence of the importance of the onset of drought for grassland vegetation as senescence marks the end of the growing season in Mediterranean grasslands (Balzarolo et al., 2015; Vescovo et al., 2012). In a previous study, Vicca (et al., 2016) found that NDWI was able to estimate GPP in semiarid grasslands better than other indices, allowing to distinguish the effect of drought.

25 Other indices, sensitive to changes in chlorophyll-a concentration, MTCI (Dash and Curran, 2004) and GNDVI (Gitelson and Merzlyak, 1998) were also included in the model. The fertilization treatment resulted in an increase in MTCI during the first stage of the experiment in the NPK and P treatments, followed by a decrease observed in all treatments as the season progressed toward the end of the annual growth cycle. A similar trend was observed in a study by (Perez-Priego et al., 2015) in which Mediterranean grasslands were subjected to fertilization with N or NP. The primary role of chlorophyll in
30 photosynthesis is well known and justifies the positive relationship observed between GPP and MTCI. However, in the present study, no differences were observed in GPP among fertilized and non-fertilized treatments suggesting that the expected increase in photosynthesis due to the increase in chlorophyll and nitrogen was constrained by other environmental and physiological factors.

Notably NDVI, the most frequently applied index in GPP estimates by LUE models (Yuan et al., 2014) was not selected in the Hyp-VIs model and showed a poorer coefficient of determination than other indices, (e.g. NDWI), NDVI is expected to mirror changes in green leaf area, being generally linearly related with fPAR (Myneni and Williams, 1994). However, previous studies reported a saturation of NDVI and consequent lack of linearity in the NDVI-fPAR regression in high

5   productive vegetation communities (Gianelle et al., 2009; Vescovo et al., 2012) such as grasslands and sometimes other indices showed a better performance. For example, in grasslands subjected to water and nutrient stress, the NDVI green index (GNDVI), which adopts a green band instead of the red band of NDVI and hence is more sensitive to chlorophyll-a concentration (Gitelson et al., 1996), showed a better performance than NDVI as fPAR proxy (Cristiano et al., 2010; Gianelle et al., 2009). Also in this study, the GNDVI explained a larger proportion of GPP variance than   NDVI in the Hyp-

10   VIs and S2-VIs models being selected in both and before NDVI in the S2-VIs model.

The indices selected by the LEAPS (i.e. NDVI, GNDVI, NDWI, MTCI, PSRI and WBI) also showed high significant relationship with GPP (tab. 4) in simple regressions explaining 63% to 72% of the variability observed. The functional convergence (Ollinger, 2011) of different traits participating in the photosynthetic process may have hampered results observed in the regression for each single vegetation index, showing a high degree of correlation for most of them (Table 4).

15   However, the selection of several VIs, representatives of different structural and functional traits in the multiple linear models and the lower performance observed in the L8 model, including solely the NDVI index, clearly indicate the importance of considering the contribution of different traits with different temporal dynamics to capture GPP temporal changes in models integrating vegetation indices.

20   **4.2 Are spectral bands better GPP estimators than VIs?**

Our results suggest that better GPP estimates can be obtained by adopting bands (Hyp-B, S2-B, L8-B, Table 5) instead of vegetation indices (Hyp-VIs, S2-VIs, L8-Vis, Table 5). Although normalized VIs are important in establishing strong relationships between biophysical and optical properties of vegetation, our results showed that the selection of the proper band is more important than the mathematical formulation of the indices for the explanatory power of spectral retrievals as

25   predictor variables. Previous studies comparing the explanatory power of VIs and bands in grasslands showed similar results (Balzarolo et al., 2015; Matthes et al., 2015).

Our results also evidenced the importance of the SWIR region of the spectra, as bands in this region were selected in all one- and two-step models, which is rarely adopted in vegetation indices with few exceptions. The SWIR region is known to correlate with canopy water content (Casas et al., 2014).

30   Studies investigating the potential of spectral bands to estimate canopy chlorophyll content and green *f*APAR, found that the SWIR region was strongly positively correlated with them in grasslands (Sakowska et al., 2016) and also GPP in a semi-arid savanna (Tagesson et al., 2015).

Bands in the red-edge region were also largely represented in the Hyp-B, S2-B and in the Hyp-VIs+B models. The red-edge corresponds to the steep increase in reflectance at the boundary between the red region where chlorophyll is absorbed and the leaf scattering at the NIR region. Red-edge bands were successfully employed for estimating chlorophyll content in maize (Zhang and Zhou, 2017), LAI in crops (Kira et al., 2017). For these reasons they were integrated into numerous VIs, such as

5   MTCI and PSRI, also applied in this study, which explain the reason for the lack of red-edge bands in the second step of the S2 model (S2-VIs+B) while strongly represented in the S2-B.

4.3 Satellite sensors as estimators of GPP

Differences in the selection of the vegetation indices among sensors had apparently no effect on the performance of the S2-

10   VIs and Hyp-VIs models (Table 5), while the limited number of available vegetation indices for the L8 resulted in a lower performance of the model.

Our results show an equal potential of S2 and L8 sensor for assessing GPP.

GPP estimates obtained simulating S2 and L8 sensors showed a similar performance in the –B and –VIs+B models, while when only VIs were adopted the S2 model had clearly a better performance than L8. These results suggest a need for testing

15   new vegetation indices adopting L8 bands.

In agreement with our results, other studies comparing linear additive models showed similar ability for estimating canopy cover and LAI adopting the S2 or L8 sensors (Korhonen et al., 2017).

An important difference between the S2 and L8 availability of wavebands is the lack of reflectance values in the red-edge region in the L8, which limited the possibility of computing VIs, such as MTCI and PSRI (Korhonen et al., 2017). However,

20   the limitation imposed by the lack of bands in the red-edge region, had apparently more importance for the -VIs model, while differences in the performance of the model between S2 and L8 decreased for –B and VIs+B models.

In this study, S2 and L8 data comparison was based only on the simulation of the respective bands not taking into consideration other factors possibly affecting sensors spectral response such as sun-sensor viewing geometry (Tagesson et al., 2015). Nonetheless, in a recent study (Korhonen et al., 2017) the comparisons of satellite data from the two platforms

25   showed no differences between S2 and L8 reflectance values in the NIR, SWIR1 and SWIR 2 bands. In other regions of the spectra, such as the green and blue bands reflectance values were considerably smaller in the S2 than in the L8 but still proportional, suggesting that comparisons between S2 and L8 simulated bands can largely be representative of the actual differences obtained by the two remote platforms.

At the same time, our results confirm the importance of performing hyperspectral measurements. Indeed, in this study, the

30   Hyp-VIs+B model showed to be superior to the corresponding S2 and L8 model with over than 80% of probabilities. The high detailed resolution and the wide range if wave bands makes hyperspectral sensors as unique in identifying regions of the spectra of high interest for representing different properties of vegetation (Porcar-Castell et al., 2015)

5. Conclusions

In agreement with previous studies(Perez-Priego et al., 2015; Rossini et al., 2012; Vicca et al., 2016), our results clearly indicate the need to integrate into GPP models spectral information representing both structural and functional traits of vegetation along the whole grasslands life cycle. Specifically, water content (NDWI), chlorophyll (MTCI, GNDVI) and the

5   ratio of chlorophyll to carotenoids (PSRI) were indicated as best predictor variables for GPP estimates. Altogether these vegetation indices describe the loss of photosynthetic pigments and efficiency and dry out of vegetation occurring and when considered together improved considerably GPP estimates in comparison with models adopting only NDVI.

Our study also confirms the importance of hyperspectral in-situ measurements for exploratory analysis of the relationship between biophysical and optical properties of vegetation providing a wide spectral range and high resolution of spectral

10   retrievals.

The hyperspectral reflectance values, together with the two-step procedure adopted for the selection of predictor variables allowed also to identify critical region of the spectra, not included in the initial selection of vegetation indices but that revealed their usefulness in estimating GPP. For example, the LEAPS two-step procedure evidenced which bands could improve significantly a model including only vegetation indices, identifying the red edge and SWIR regions of the spectra as

15   of major importance for improving GPP estimates. This information can be critical in the development of new spectral indices and sensors.

Our results also evidenced the potential of S2 and L8 sensor in assessing GPP, since models obtained by simulating bands from the two sensors showed similar performance. The possibility of using remote sensing information for monitoring and modelling vegetation at a suitable spatial resolution, such as in S2 and L8 sensor, allows attempted vegetation monitoring

20   and modelling in a cost-effective way, in support of sustainable agriculture management practice.

Author Contribution

S Cerasoli designed the experiment and together with Joana Faria performed field measurements. M.L. Campagnolo developed the LEAPS code. C. Nogueira and M.Caldeira set up the experimental plots. S.Cerasoli prepared the manuscript

25   with contributions from all the authors.

Acknowledgments

This work was funded by Fundação para a Ciência e a Tecnologia, ministry of Science and education, through the project MEDSPEC, Monitoring Gross Primary productivity in Mediterranean oak woodlands through remote sensing and biophysical modelling . Sofia Cerasoli is post-doc fellow (BPD/SFRH/78998/2011), Carla Nogueira is the recipiente of a

30   PhD Grant (SFRH/BD/88650/2012). Authors wish to thank Georg Wohlfarth for a critical reading of the manuscript and Joaquim Mendes, Madalena Silva, Lurdes Marçal, Alicia Horta and Paula Pais for technical help in the field and laboratory. Authors are also grateful to FLAD/NSF for funding (A1/Proj 124/12) and to the Companhia das Lezírias for providing access to the grassland site and permission to undertake research.

35

References

Aires, L. M., Pio, C. A. and Pereira, J. S.: The effect of drought on energy and water vapour exchange above a mediterranean C3/C4 grassland in Southern Portugal, Agric. For. Meteorol., 148(4), 565–579, doi:10.1016/j.agrformet.2007.11.001, 2008a.

Aires, L. M. I., Pio, C. A. and Pereira, J. S.: Carbon dioxide exchange above a Mediterranean C3/C4 grassland during two climatologically contrasting years, Glob. Chang. Biol., 14(3), 539–555, doi:10.1111/j.1365-2486.2007.01507.x, 2008b.

Balzarolo, M., Vescovo, L., Hammerle, A., Gianelle, D., Papale, D., Tomelleri, E. and Wohlfahrt, G.: On the relationship between ecosystem-scale hyperspectral reflectance and CO_2 exchange in European mountain grasslands, Biogeosciences, 12(10), 3089–3108, doi:10.5194/bg-12-3089-2015, 2015.

Barsi, J., Lee, K., Kvaran, G., Markham, B. and Pedelty, J.: The Spectral Response of the Landsat-8 Operational Land Imager, Remote Sens., 6(10), 10232–10251, doi:10.3390/rs61010232, 2014.

Bates, D., Mächler, M., Bolker, B. and Walker, S.: Fitting Linear Mixed-Effects Models using lme4, J. Stat. Softw., 67(1), 1–48, doi:10.18637/jss.v067.i01, 2014.

Beer, C., Reichstein, M., Tomelleri, E., Ciais, P., Jung, M., Carvalhais, N., Rödenbeck, C., Arain, M. A., Baldocchi, D., Bonan, G. B., Bondeau, A., Cescatti, A., Lasslop, G., Lindroth, A., Lomas, M., Luyssaert, S., Margolis, H., Oleson, K. W., Roupsard, O., Veenendaal, E., Viovy, N., Williams, C., Woodward, F. I. and Papale, D.: Terrestrial gross carbon dioxide uptake: global distribution and covariation with climate., Science, 329(5993), 834–838, doi:10.1126/science.1184984, 2010.

Borer, E. T., Grace, J. B., Harpole, W. S., MacDougall, A. S. and Seabloom, E. W.: A decade of insights into grassland ecosystem responses to global environmental change, Nat. Ecol. Evol., 1(5), 118, doi:10.1038/s41559-017-0118, 2017.

Bugalho, M. N. and Abreu, J. M.: The multifunctional role of grasslands, in Sustainable Mediterranean Grasslands and their Multifunctions. vol. 79. Option Méditerraneénes, edited by C. Porqueddu and M. M. Tavares de Sousa, pp. 25–30., 2008.

Casas, A., Riaño, D., Ustin, S. L., Dennison, P. and Salas, J.: Estimation of water-related biochemical and biophysical vegetation properties using multitemporal airborne hyperspectral data and its comparison to MODIS spectral response, Remote Sens. Environ., 148, 28–41, doi:10.1016/j.rse.2014.03.011, 2014.

Ceulemans, T., Stevens, C. J., Duchateau, L., Jacquemyn, H., Gowing, D. J. G., Merckx, R., Wallace, H., van Rooijen, N., Goethem, T., Bobbink, R., Dorland, E., Gaudnik, C., Alard, D., Corcket, E., Muller, S., Dise, N. B., Dupré, C., Diekmann, M. and Honnay, O.: Soil phosphorus constrains biodiversity across European grasslands, Glob. Chang. Biol., 20(12), 3814–3822, doi:10.1111/gcb.12650, 2014.

Cheng, Y.-B., Zhang, Q., Lyapustin, A. I., Wang, Y. and Middleton, E. M.: Impacts of light use efficiency and fPAR parameterization on gross primary production modeling, Agric. For. Meteorol., 189–190, 187–197, doi:10.1016/j.agrformet.2014.01.006, 2014.

Costa, A. C., Santos, J. A. and Pinto, J. G.: Climate change scenarios for precipitation extremes in Portugal, Theor. Appl. Climatol., 108(1–2), 217–234, doi:10.1007/s00704-011-0528-3, 2012.

Cristiano, P. M., Posse, G., Di Bella, C. M. and Jaimes, F. R.: Uncertainties in fPAR estimation of grass canopies under

different stress situations and differences in architecture, Int. J. Remote Sens., 31, 4095–4109, doi:10.1080/01431160903229192, 2010.

Dash, J. and Curran, P. J.: The MERIS terrestrial chlorophyll index, Int. J. Remote Sens., 25(23), 5403–5413, doi:10.1080/0143116042000274015, 2004.

5 Díaz-Villa, M. D., Marañón, T., Arroyo, J. and Garrido, B.: Soil seed bank and floristic diversity in a forest-grassland mosaic in southern Spain, J. Veg. Sci., 14(5), 701–709, doi:10.1111/j.1654-1103.2003.tb02202.x, 2003.

Drusch, M., Del Bello, U., Carlier, S., Colin, O., Fernandez, V., Gascon, F., Hoersch, B., Isola, C., Laberinti, P., Martimort, P., Meygret, A., Spoto, F., Sy, O., Marchese, F. and Bargellini, P.: Sentinel-2: ESA's Optical High-Resolution Mission for GMES Operational Services, Remote Sens. Environ., 120, 25–36, doi:10.1016/j.rse.2011.11.026, 2012.

10 ESA: Sentinel-2 Data Quality Report Issue 24 (February 2018) - Sentinel-2 MSI Document Library - User Guides - Sentinel Online, [online] Available from: https://earth.esa.int/web/sentinel/user-guides/sentinel-2-msi/document-library/ (Accessed 25 January 2018), 2018.

Fensholt, R., Sandholt, I. and Rasmussen, M. S.: Evaluation of MODIS LAI, fAPAR and the relation between fAPAR and NDVI in a semi-arid environment using in situ measurements, Remote Sens. Environ., 91, 490–507, 15 doi:10.1016/j.rse.2004.04.009, 2004.

Filella, I., Peñuelas, J., Llorens, L. and Estiarte, M.: Reflectance assessment of seasonal and annual changes in biomass and CO_2 uptake of a Mediterranean shrubland submitted to experimental warming and drought, Remote Sens. Environ., 90(3), 308–318, doi:10.1016/j.rse.2004.01.010, 2004.

Filella, I., Porcar-Castell, A., Munné-Bosch, S., Bäck, J., Garbulsky, M. F. and Peñuelas, J.: PRI assessment of long-term 20 changes in carotenoids/chlorophyll ratio and short-term changes in de-epoxidation state of the xanthophyll cycle, Int. J. Remote Sens., 30(17), 4443–4455, doi:10.1080/01431160802575661, 2009.

Filippa, G., Cremonese, E., Migliavacca, M., Galvagno, M., Forkel, M., Wingate, L., Tomelleri, E., Morra di Cella, U. and Richardson, A. D.: Phenopix: A R package for image-based vegetation phenology, Agric. For. Meteorol., 220, 141–150, doi:10.1016/j.agrformet.2016.01.006, 2016.

25 Furnival, G. M. and Wilson, R. W.: Regressions by Leaps and Bounds, Technometrics, 16(4), 499–511, doi:10.1080/00401706.1974.10489231, 1974.

Galloway, J. N., Dentener, F. J., Capone, D. G., Boyer, E. W., Howarth, R. W., Seitzinger, S. P., Asner, G. P., Cleveland, C. C., Green, P. A., Holland, E. A., Karl, D. M., Michaels, A. F., Porter, J. H., Townsend, A. R. and Vosmarty, C. J.: Nitrogen Cycles: Past, Present, and Future, Biogeochemistry, 70(2), 153–226, doi:10.1007/s10533-004-0370-0, 2004.

30 Gamon, J. A.: Reviews and Syntheses: optical sampling of the flux tower footprint, Biogeosciences, 12(14), 4509–4523, doi:10.5194/bg-12-4509-2015, 2015.

Gamon, J. A., Penuelas, J. and Field, C. B.: A narrow-wave band spectral index that tracks diurnal changes in photosynthetic efficiency, Remote Sens. Environ., 41(1), 35–44, 1992.

Gamon, J. A., Serrano, L. and Surfus, J. S.: The photochemical reflectance index: an optical indicator of photosynthetic

radiation use efficiency across species, functional types, and nutrient levels, Oecologia, 112, 492–501, doi:10.1007/s004420050337, 1997.

Gao, B.: NDWI—A normalized difference water index for remote sensing of vegetation liquid water from space, Remote Sens. Environ., 58(3), 257–266, doi:10.1016/S0034-4257(96)00067-3, 1996.

5 Gianelle, D., Vescovo, L., Marcolla, B., Manca, G. and Cescatti, A.: Ecosystem carbon fluxes and canopy spectral reflectance of a mountain meadow, Int. J. Remote Sens., 30(2), 435–449, doi:10.1080/01431160802314855, 2009.

Gitelson, A. and Merzlyak, M. N.: Spectral reflectance changes associated with autumn senescence of Aesculus-Hippocastanum L. and Acer-Platanoides L leaves - spectral features and relation to chlorophyll estimation, J. Plant Physiol., 143, 286–292, 1994.

10 Gitelson, A. A. and Merzlyak, M. N.: Remote sensing of chlorophyll concentration in higher plant leaves, Adv. Sp. Res., 22, 689–692, doi:http://dx.doi.org/10.1016/S0273-1177(97)01133-2, 1998.

Gitelson, A. A., Kaufman, Y. J. and Merzlyak, M. N.: Use of a green channel in remote sensing of global vegetation from EOS-MODIS, Remote Sens. Environ., 58(3), 289–298, doi:10.1016/S0034-4257(96)00072-7, 1996.

Gitelson, A. A., Gamon, J. A. and Solovchenko, A.: Multiple drivers of seasonal change in PRI: Implications for
15 photosynthesis 1. Leaf level, Remote Sens. Environ., 191, 110–116, doi:10.1016/j.rse.2016.12.014, 2017a.

Gitelson, A. A., Gamon, J. A. and Solovchenko, A.: Multiple drivers of seasonal change in PRI: Implications for photosynthesis 2. Stand level, Remote Sens. Environ., 190, 198–206, doi:10.1016/J.RSE.2016.12.015, 2017b.

Gower, S. T., Kucharik, C. J. and Norman, J. M.: Direct and Indirect Estimation of Leaf Area Index, fAPAR, and Net Primary Production of Terrestrial Ecosystems, Remote Sens. Environ., 70, 29–51, doi:10.1016/S0034-4257(99)00056-5,
20 1999.

Grimm, N. B., Grove, J. M., Pickett, S. T. a and Redman, C. L.: Integrated approaches to long-term studies of urban ecological systems, Bioscience, 50(7), 571–584, doi:10.1641/0006-3568, 2008.

Harpole, W. S., Potts, D. L. and Suding, K. N.: Ecosystem responses to water and nitrogen amendment in a California grassland, Glob. Chang. Biol., 13(11), 2341–2348, doi:10.1111/j.1365-2486.2007.01447.x, 2007.

25 Hothorn, T., Bretz, F. and Westfall, P.: Simultaneous Inference in General Parametric Models, Biometrical J., 50(3), 346–363, doi:10.1002/bimj.200810425, 2008.

INMG: O clima de Portugal. Normais climatológicas da região Ribatejo e Oeste correspondentes a 1951-1980., 1991.

Joel, G., Gamon, J. A. and Field, C. B.: Production efficiency in sunflower: The role of water and nitrogen stress, Remote Sens. Environ., 62, 176–188, doi:10.1016/s0034-4257(97)00093-x, 1997.

30 Jongen, M., Unger, S., Fangueiro, D., Cerasoli, S., Silva, J. M. N. and Pereira, J. S.: Resilience of montado understorey to experimental precipitation variability fails under severe natural drought, Agric. Ecosyst. Environ., 178, 18–30, 2013.

Kira, O., Nguy-Robertson, A. L., Arkebauer, T. J., Linker, R. and Gitelson, A. A.: Toward generic models for green LAI estimation in maize and soybean: Satellite observations, Remote Sens., 9(4), 318, doi:10.3390/rs9040318, 2017.

Korhonen, L., Hadi, Packalen, P. and Rautiainen, M.: Comparison of Sentinel-2 and Landsat 8 in the estimation of boreal

forest canopy cover and leaf area index, Remote Sens. Environ., 195, 259–274, doi:10.1016/j.rse.2017.03.021, 2017.

Kovats, R. S., Valentini, R., Bouwer, L. M., Georgopoulou, E., Jacob, D., Martin, E. and Rounsevell, M. Soussana, J. F.: Europe, in Climate Change 2014: Impacts, Adaptation, and Vulnerability. Part B: Regional Aspects. Contribution of Working Group II to the Fifth Assessment Report of the Intergovernmental Panel on Climate Change, pp. 1267–1326, Cambridge University Press, Cambridge, United Kingdom and New York, NY, USA., 2014.

Loveland, T. R. and Irons, J. R.: Landsat 8: The plans, the reality, and the legacy, Remote Sens. Environ., 185, 1–6, doi:10.1016/j.rse.2016.07.033, 2016.

Lumley, T.: Thomas Lumley using Fortran code by Alan Miller (2009). Leaps: regression subset selection. R package version 2.9., 2009.

Matthes, J. H., Knox, S. H., Sturtevant, C., Sonnentag, O., Verfaillie, J. and Baldocchi, D.: Predicting landscape-scale CO_2 flux at a pasture and rice paddy with long-term hyperspectral canopy reflectance measurements, Biogeosciences, 12(15), 4577–4594, doi:10.5194/bg-12-4577-2015, 2015.

Merzlyak, M. N., Gitelson, A. A., Chivkunova, O. B. and Rakitin, V. Y.: Non-destructive optical detection of pigment changes during leaf senescence and fruit ripening, Physiol. Plant., 106(1), 135–141, doi:10.1034/j.1399-3054.1999.106119.x, 1999.

Monteith, J. L.: Solar Radiation and Productivity in Tropical Ecosystems, J. Appl. Ecol., 9(3), 747–766, doi:10.2307/2401901, 1972.

Monteith, J. L.: Climate and efficiency of crop production in Britain, Philos. Trans. R. Soc. London Ser. B-Biological Sci., 281, 277–294, 1977.

Moreno, A., Maselli, F., Gilabert, M. A., Chiesi, M., Martinez, B. and Seufert, G.: Assessment of MODIS imagery to track light-use efficiency in a water-limited Mediterranean pine forest, Remote Sens. Environ., 123, 359–367, doi:10.1016/j.rse.2012.04.003, 2012.

Myneni, R. B. and Williams, D. L.: On the relationship between FAPAR and NDVI, Remote Sens. Environ., 49(3), 200–211, 1994.

Naudts, K., Chen, Y., McGrath, M. J., Ryder, J., Valade, A., Otto, J. and Luyssaert, S.: Europes forest management did not mitigate climate warming, Science (80-.)., 351(6273), 597–600, doi:10.1126/science.aad7270, 2016.

Nestola, E., Calfapietra, C., Emmerton, C. A., Wong, C. Y. S., Thayer, D. R. and Gamon, J. A.: Monitoring grassland seasonal carbon dynamics, by integrating MODIS NDVI, proximal optical sampling, and eddy covariance measurements, Remote Sens., 8(3), 260, doi:10.3390/rs8030260, 2016.

Ohtani, K.: Bootstrapping R2 and adjusted R2 in regression analysis, Econ. Model., 17(4), 473–483, doi:10.1016/S0264-9993(99)00034-6, 2000.

Ollinger, S. V.: Sources of variability in canopy reflectance and the convergent properties of plants, New Phytol., 189(2), 375–394, doi:10.1111/j.1469-8137.2010.03536.x, 2011.

Penuelas, J., Pinol, J., Ogaya, R. and Filella, I.: Estimation of plant water concentration by the reflectance Water Index WI

(R900/R970), Int. J. Remote Sens., 18(13), 2869–2875, doi:10.1080/014311697217396, 1997.

Peñuelas, J., Filella, I. and Gamon, J. A.: Assessment of photosynthetic radiation-use efficiency with spectral reflectance, New Phytol., 131(3), 291–296, doi:10.1111/j.1469-8137.1995.tb03064.x, 1995.

Peñuelas, J., Poulter, B., Sardans, J., Ciais, P., van der Velde, M., Bopp, L., Boucher, O., Godderis, Y., Hinsinger, P., Llusia, J., Nardin, E., Vicca, S., Obersteiner, M. and Janssens, I. A.: Human-induced nitrogen–phosphorus imbalances alter natural and managed ecosystems across the globe, Nat. Commun., 4, 2934, doi:10.1038/ncomms3934, 2013.

Penuelas et al., J.: The reflectance at the 950-970nm region as an indicator of plant water status, Int. J. Remote Sens., 14(10), 1887–1905, doi:0143-1161/93, 1993.

Perez-Priego, O., Guan, J., Rossini, M., Fava, F., Wutzler, T., Moreno, G., Carvalhais, N., Carrara, A., Kolle, O., Julitta, T., Schrumpf, M., Reichstein, M. and Migliavacca, M.: Sun-induced chlorophyll fluorescence and photochemical reflectance index improve remote-sensing gross primary production estimates under varying nutrient availability in a typical Mediterranean savanna ecosystem, Biogeosciences, 12(21), 6351–6367, doi:10.5194/bg-12-6351-2015, 2015.

Pérez-Priego, O., López-Ballesteros, A., Sánchez-Cañete, E. P., Serrano-Ortiz, P., Kutzbach, L., Domingo, F., Eugster, W. and Kowalski, A. S.: Analysing uncertainties in the calculation of fluxes using whole-plant chambers: random and systematic errors, Plant Soil, 393(1–2), 229–244, doi:10.1007/s11104-015-2481-x, 2015.

Porcar-Castell, A., Garcia-Plazaola, J. I., Nichol, C. J., Kolari, P., Olascoaga, B., Kuusinen, N., Fernandez-Marin, B., Pulkkinen, M., Juurola, E. and Nikinmaa, E.: Physiology of the seasonal relationship between the photochemical reflectance index and photosynthetic light use efficiency, Oecologia, 170(2), 313–323, doi:10.1007/s00442-012-2317-9, 2012.

Porcar-Castell, A., Mac Arthur, A., Rossini, M., Eklundh, L., Pacheco-Labrador, J., Anderson, K., Balzarolo, M., Martín, M. P., Jin, H., Tomelleri, E., Cerasoli, S., Sakowska, K., Hueni, A., Julitta, T., Nichol, C. J. and Vescovo, L.: EUROSPEC: at the interface between remote-sensing and ecosystem CO_2 flux measurements in Europe, Biogeosciences, 12(20), 6103–6124, doi:10.5194/bg-12-6103-2015, 2015.

Rossini, M., Cogliati, S., Meroni, M., Migliavacca, M., Galvagno, M., Busetto, L., Cremonese, E., Julitta, T., Siniscalco, C., Morra di Cella, U. and Colombo, R.: Remote sensing-based estimation of gross primary production in a subalpine grassland, Biogeosciences, 9(7), 2565–2584, doi:10.5194/bg-9-2565-2012, 2012.

Rouse, J. W., Haas, R. H., Schell, J. A. and Deering, D. W.: Monitoring vegetation systems in the great plains with ERTS, in Third ERTS Symposium, vol. 1, edited by N. SP-351, pp. 309–317, NASA, Washington, DC, USA., 1974.

Sakowska, K., Vescovo, L., Marcolla, B., Juszczak, R., Olejnik, J. and Gianelle, D.: Monitoring of carbon dioxide fluxes in a subalpine grassland ecosystem of the Italian Alps using a multispectral sensor, Biogeosciences, 11, 4695–4712, doi:10.5194/bg-11-4695-2014, 2014.

Sakowska, K., Juszczak, R. and Gianelle, D.: Remote Sensing of Grassland Biophysical Parameters in the Context of the Sentinel-2 Satellite Mission, J. Sensors, 2016, 1–16, doi:10.1155/2016/4612809, 2016.

Sala, O. E.: Global Biodiversity Scenarios for the Year 2100, Science (80-.)., 287(5459), 1770 LP-1774, 2000.

Schimel, D., Pavlick, R., Fisher, J. B., Asner, G. P., Saatchi, S., Townsend, P., Miller, C., Frankenberg, C., Hibbard, K. and

Cox, P.: Observing terrestrial ecosystems and the carbon cycle from space, Glob. Chang. Biol., 21(5), 1762–1776, doi:10.1111/gcb.12822, 2015.

Seabloom, E. W., Borer, E. T., Buckley, Y., Cleland, E. E., Davies, K., Firn, J., Harpole, W. S., Hautier, Y., Lind, E., MacDougall, A., Orrock, J. L., Prober, S. M., Adler, P., Alberti, J., Michael Anderson, T., Bakker, J. D., Biederman, L. A., Blumenthal, D., Brown, C. S., Brudvig, L. A., Caldeira, M., Chu, C., Crawley, M. J., Daleo, P., Damschen, E. I., D'Antonio, C. M., DeCrappeo, N. M., Dickman, C. R., Du, G., Fay, P. A., Frater, P., Gruner, D. S., Hagenah, N., Hector, A., Helm, A., Hillebrand, H., Hofmockel, K. S., Humphries, H. C., Iribarne, O., Jin, V. L., Kay, A., Kirkman, K. P., Klein, J. A., Knops, J. M. H., La Pierre, K. J., Ladwig, L. M., Lambrinos, J. G., Leakey, A. D. B., Li, Q., Li, W., McCulley, R., Melbourne, B., Mitchell, C. E., Moore, J. L., Morgan, J., Mortensen, B., O'Halloran, L. R., Pärtel, M., Pascual, J., Pyke, D. A., Risch, A. C., Salguero-Gómez, R., Sankaran, M., Schuetz, M., Simonsen, A., Smith, M., Stevens, C., Sullivan, L., Wardle, G. M., Wolkovich, E. M., Wragg, P. D., Wright, J. and Yang, L.: Predicting invasion in grassland ecosystems: is exotic dominance the real embarrassment of richness?, Glob. Chang. Biol., 19(12), 3677–3687, doi:10.1111/gcb.12370, 2013.

Tagesson, T., Fensholt, R., Huber, S., Horion, S., Guiro, I., Ehammer, A. and Ardö, J.: Deriving seasonal dynamics in ecosystem properties of semi-arid savanna grasslands from in situ-based hyperspectral reflectance, Biogeosciences, 12(15), 4621–4635, doi:10.5194/bg-12-4621-2015, 2015.

Thomas, H.: Senescence, ageing and death of the whole plant, New Phytol., 197(3), 696–711, doi:10.1111/nph.12047, 2013.

Vescovo, L., Wohlfahrt, G., Balzarolo, M., Pilloni, S., Sottocornola, M., Rodeghiero, M. and Gianelle, D.: New spectral vegetation indices based on the near-infrared shoulder wavelengths for remote detection of grassland phytomass, Int. J. Remote Sens., 33(7), 2178–2195, doi:10.1080/01431161.2011.607195, 2012.

Vicca, S., Balzarolo, M., Filella, I., Granier, A., Herbst, M., Knohl, A., Longdoz, B., Mund, M., Nagy, Z., Pintér, K., Rambal, S., Verbesselt, J., Verger, A., Zeileis, A., Zhang, C. and Peñuelas, J.: Remotely-sensed detection of effects of extreme droughts on gross primary production, Sci. Rep., 6(1), 28269, doi:10.1038/srep28269, 2016.

Viña, A. and Gitelson, A. A.: New developments in the remote estimation of the fraction of absorbed photosynthetically active radiation in crops, Geophys. Res. Lett., 32(17), doi:10.1029/2005GL023647, 2005.

WRB, I. W. G.: World reference base for soil resources 2006. 2nd edition. World Soil Resources Reports No.103 ., 2006.

Xu, L. and Baldocchi, D. D.: Seasonal variation in carbon dioxide exchange over a Mediterranean annual grassland in California, Agric. For. Meteorol., 123(1–2), 79–96, doi:10.1016/j.agrformet.2003.10.004, 2004.

Yuan, W., Cai, W., Xia, J., Chen, J., Liu, S., Dong, W., Merbold, L., Law, B., Arain, A., Beringer, J., Bernhofer, C., Black, A., Blanken, P. D., Cescatti, A., Chen, Y., Francois, L., Gianelle, D., Janssens, I. A., Jung, M., Kato, T., Kiely, G., Liu, D., Marcolla, B., Montagnani, L., Raschi, A., Roupsard, O., Varlagin, A. and Wohlfahrt, G.: Global comparison of light use efficiency models for simulating terrestrial vegetation gross primary production based on the LaThuile database, Agric. For. Meteorol., 192–193, 108–120, doi:10.1016/j.agrformet.2014.03.007, 2014.

Zhang, F. and Zhou, G.: Deriving a light use efficiency estimation algorithm using *in situ* hyperspectral and eddy covariance measurements for a maize canopy in Northeast China, Ecol. Evol., 7(13), 4735–4744, doi:10.1002/ece3.3051, 2017.

Table 1. Spectral bands range and spatial resolution of Sentinel-2A MSI and Landsat 8 OLI sensors simulated in this study.

Band	Sentinel-2A MSI			Landsat 8 OLI		
	Spectral region	Wavelength range (nm)	Resolution (m)	Spectral region	Wavelength range (nm)	Resolution (m)
B1				Blue	435-451	30
B2	Blue	458-523	10	Blue	452-512	30
B3	Green peak	543-578	10	Green	533-590	30
B4	red	650-680	10	Red	636-673	30
B5	Red-edge	698-713	20	NIR	851-879	30
B6	Red-edge	733-748	20	SWIR1	1566-1651	30
B7	Red-edge	773-793	20	SWIR2	2107-2294	30
B8	NIR	785-899	10			
B8A	NIR narrow	855-875	20			
B11	SWIR	1565-1655	20			
B12	SWIR	2100-2280	20			

Table 2. Selection of vegetation indices adopted in this study with their formulation using hyperspectral (Hyp) grouped bands, S2 or L8 simulated sensors, biophysical properties represented according to the literature and original bibliographic reference.

	Vegetation Index	Hyp	S2	L8	Biophysical property	Reference
NDVI	Normalized Difference Vegetation Index	$\dfrac{R_{800} - R_{670}}{R_{800} + R_{670}}$	$\dfrac{B8A - B4}{B8A + B4}$	$\dfrac{B5 - B4}{B5 + B4}$	Green biomass and area	(Rouse et al., 1974)
GNDVI	Green Normalized Diff. Veg. Ind.	$\dfrac{R_{750} - R_{550}}{R_{750} + R_{550}}$	$\dfrac{B7 - B3}{B7 + B3}$	$\dfrac{B5 - B3}{B5 + B3}$	Green biomass and area	(Gitelson and Merzlyak, 1998)
NDVIre	Red-edge Normalized Diff. Veg. Ind.	$\dfrac{R_{750} - R_{720}}{R_{720} + R_{750}}$			Green biomass	(Gitelson and Merzlyak, 1994)
CI	Chlorophyll index	$\dfrac{R_{750} - R_{705}}{R_{750} + R_{705}}$			Chlorophyll	(Gitelson and Merzlyak, 1994)
MTCI	MERIS Terrestrial chlorophyll Index	$\dfrac{R_{754} - R_{709}}{R_{709} + R_{681}}$	$\dfrac{B6 - B5}{B5 + B4}$		Chlorophyll, nitrogen	(Dash and Curran, 2004)
PRI	Photochemical Reflectance Index	$\dfrac{R_{570} - R_{531}}{R_{570} + R_{531}}$			Radiation Use-Efficiency, Carotenoid/chlorophyll	(Gamon et al., 1992)
PSRI	Plant Senescence Reflectance Index	$\dfrac{R_{680} - R_{500}}{R_{750}}$	$\dfrac{B4 - B3}{B6}$		Carotenoid/chlorophyll	(Merzlyak et al., 1999)
NDWI	Normalized Difference Water Index	$\dfrac{R_{860} - R_{1240}}{R_{860} + R_{1240}}$			Tissue water content	(Gao, 1996)
WBI	Water Band Index	$\dfrac{R_{970} - R_{900}}{R_{970} + R_{900}}$			Tissue water content	(Penuelas et al., 1993)

Tab.3 - Percentage of each plant functional type (Forbs, Graminoids and Legumes) in above ground biomass of grasslands under different fertilization treatments (C, N, NPK and P). Values represent means of 6 replicates; standard errors are shown in parenthesis.

Treatment	Forbs	Grams	Legumes
C	56.85	21.22	21.93
	(5.10)	(3.62)	(4.20)
N	65.00	25.04	9.95
	(1.89)	(2.53)	(1.45)
NPK	34.07	52.55	13.37
	(3.43)	(3.29)	(1.03)
P	25.60	31.43	42.96
	(3.06)	(4.47)	(3.82)

Table 4. Linear regressions established between lnGPP and vegetation indices (VI) selected for this study (see Table 2). Best regression is shown in bold.

Vegetation Index	R^2	RMSE	P
NDVI	0.6853	0.2364	0.0000
GNDVI	0.6360	0.2543	0.0000
NDVIre	0.6872	0.2357	0.0000
CI	0.7161	0.2246	0.0000
MTCI	0.6303	0.2563	0.0000
PRI	0.0209	0.4171	0.1715
PSRI	0.6745	0.2405	0.0000
NDWI	**0.7205**	**0.2228**	**0.0000**
WBI	0.6491	0.2497	0.0000

Table 5. Best selection of linear models for GPP estimate according to the general equation: $lnGPPP \sim \sum_{j,1}^{n} vj$, where v are vegetation indices (VIs) or optical bands (B). Bands and vegetation indices are obtained from Hyperspectral measurements grouped in clusters with 90% similarity (Hyp), or resampled for simulating Sentinel 2/MSI (S2) and Landsat8/OLI (L8) sensors. Vegetation indices formulation is shown in Table 2. The order of the variables (most important first) reflects their importance in the model. The Quantiles 25% and 75% of the *adj R^2* are obtained from a bootstrap with 10000 iterations. The two-steps models add a selection of bands to the variables (VIs) selected at step one. A low p-value indicates that the model including VIs and bands (step 2) is significantly better than the model just with VIs (step 1).

Model	Step one	Adj R^2	Adj R^2 Q-25%	Adj R^2 Q-75%	Step two	Adj R^2	Adj R^2 Q 25%	Adj R^2 Q75%	p
Hyp-VIs	NDWI; PSRI; WBI; GNDVI	0.7659	0.7431	0.8047					
S2-VIs	MTCI; PSRI; GNDVI; NDVI	0.7426	0.7225	0.7822					
L8-VIs	NDVI	0.6792	0.6405	0.7194					
Hyp-B	$R_{1951-2299}$; $R_{724-732}$; $R_{1328-1349}$; $R_{706-710}$; $R_{449-466}$; $R_{566-582}$; $R_{519-532}$; $R_{350-397}$; $R_{398-411}$; $R_{1209-1327}$; $R_{702-705}$; $R_{698-701}$; $R_{716-723}$;	0.7884	0.7906	0.8392					
S2-B	B7; B11; B5; B2; B8; B6	0.7412	0.7222	0.7848					
L8-B	B7; B5; B6; B4; B3; B1	0.7557	0.7367	0.7974					
Hyp-VIs+B	NDWI; PSRI; WBI; GNDVI				$R_{698-701}$; $R_{412-448}$; $R_{716-723}$; $R_{467-518}$; $R_{706-710}$; $R_{449-466}$; $R_{350-397}$; $R_{1209-1327}$; $R_{1412-1505}$; $R_{1951-2299}$; $R_{702-705}$; $R_{724-732}$; $R_{1328-1349}$	0.7986	0.8083	0.8550	0.0260
S2-VIs+B	MTCI; PSRI; GNDVI; NDVI				B11; B3; B12	0.7684	0.7542	0.8104	0.0081
L8-VIs+B	NDVI				B6; B3; B7	0.7686	0.7472	0.8047	0.0000
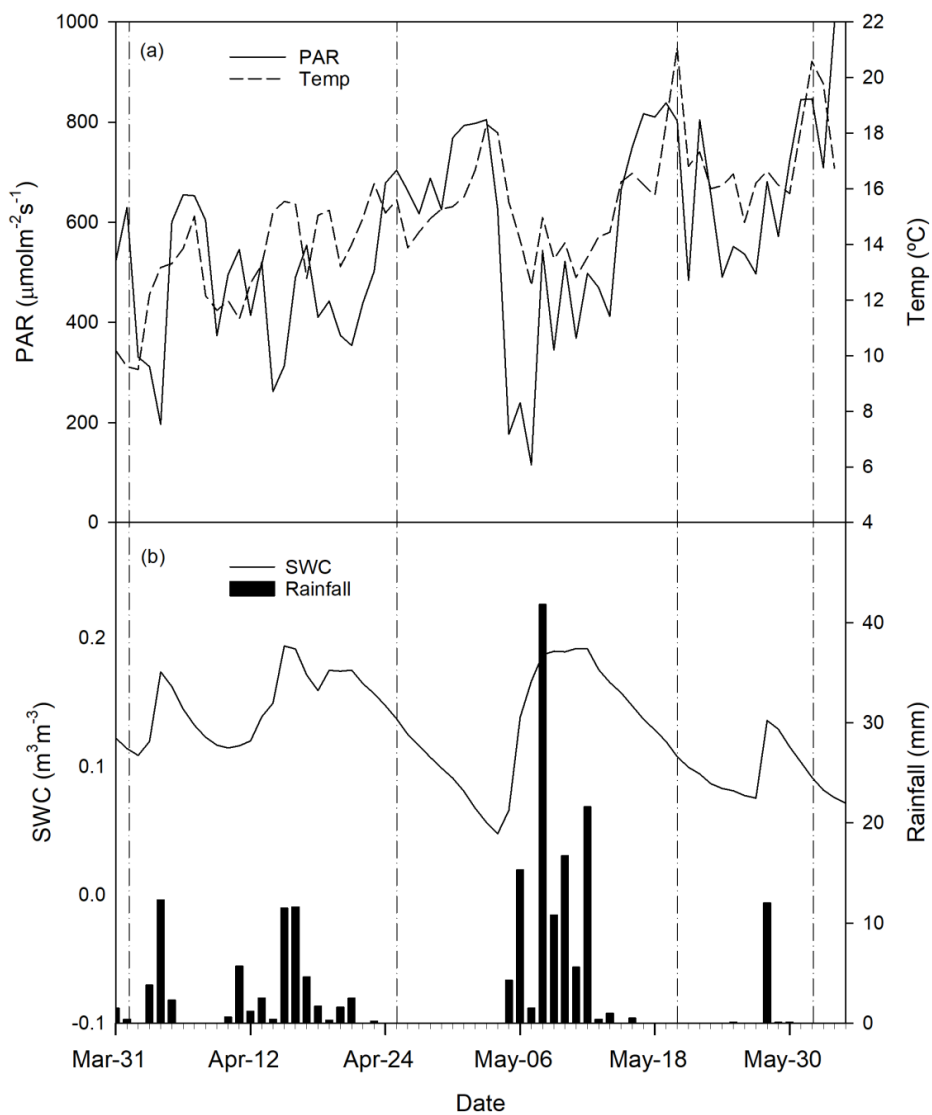
Figure 1: Daily average PAR, temperature (a), soil water content for different treatments and total rainfall (b) recorded on the site during the experimental period. Dates of field measurements are indicated by vertical dash-dotted lines.
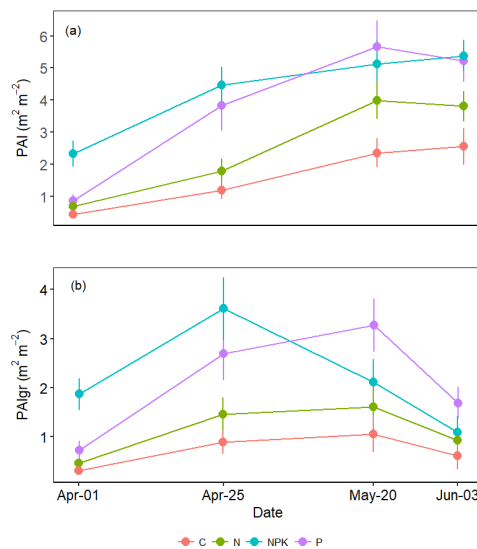
Figure 2 Average green Plant Area index (PAI) and the green fraction of PAI (PAIgr) observed in grasslands subjected to different fertilization treatments (C, N, NPK or P). Each point is the average of 6 replicates. Vertical bars represent error bars.
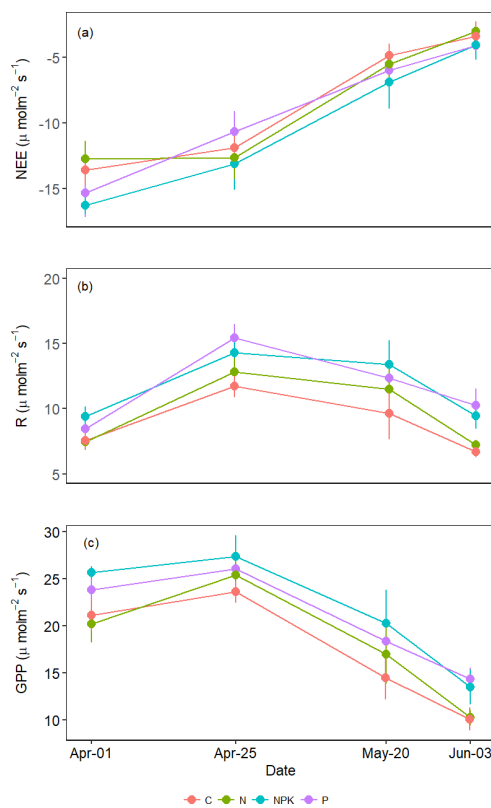
Fig.3 Average Net Ecosystem Exchange (NEE)(a), dark Respiration (R) (b) and Gross Primary Productivity (GPP) (c) measured in grasslands under different fertilization regimes (C, N, NPK and P). Each point is the average of 6 replicates. Vertical bars represent standard errors.
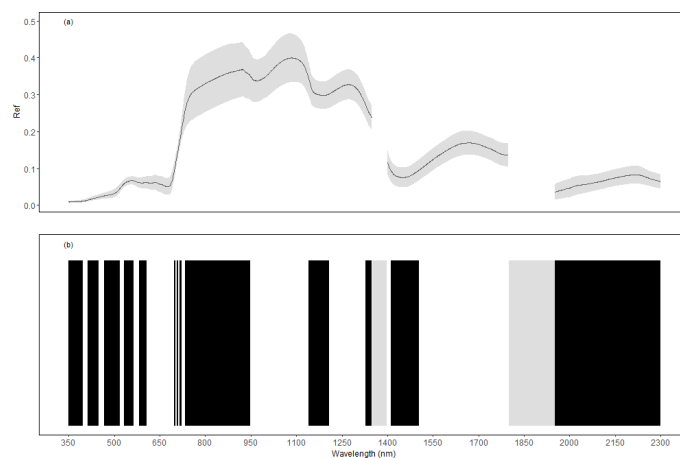
Fig.4 Average reflectance values and standard deviation (grey ribbon) observed in herbaceous plots undergoing different fertilization treatments (A). The bottom picture (B) shows the bands obtained by grouping Ref for similarity (>=90%) of contiguous hyperspectral measurements with 1nm resolution in the range 350-2300nm, bands are alternated black and white. Grey bars represent areas of the spectrum not considered for being noise.
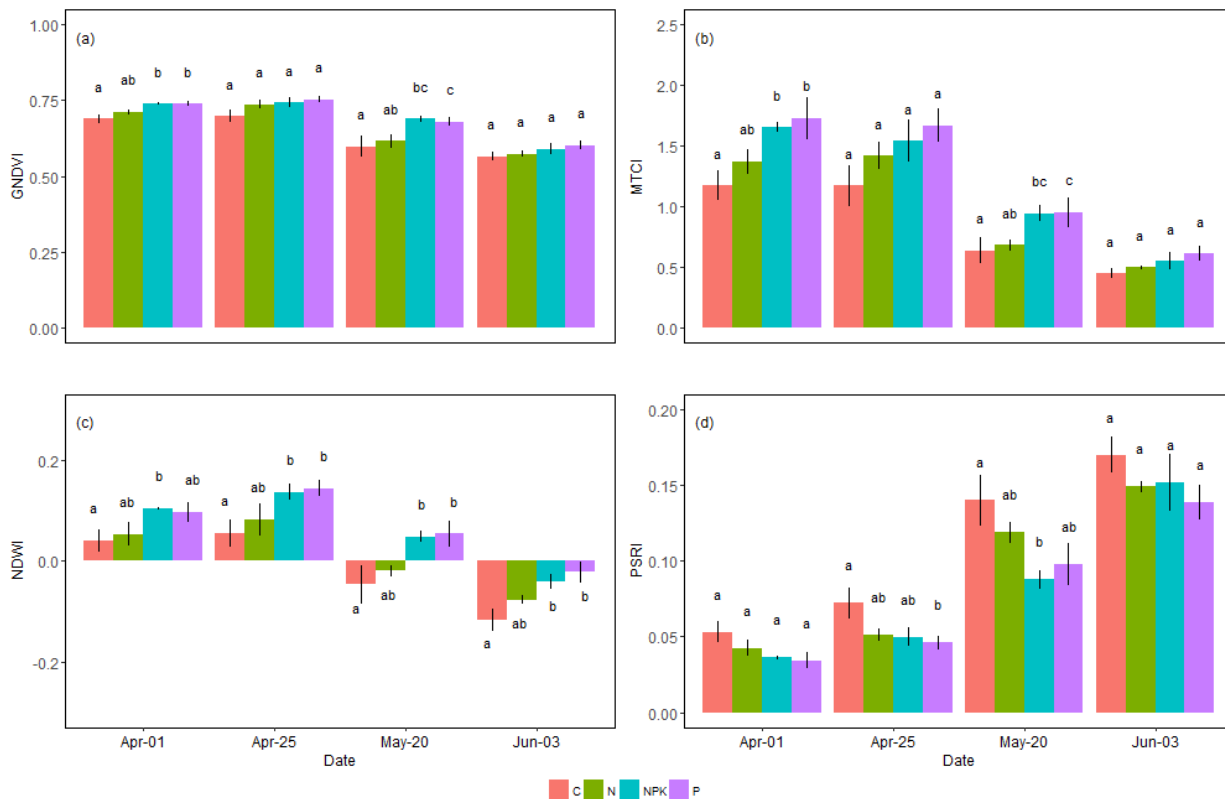
Fig 5. Average values of several vegetation indices retrieved from reflectance measurements of herbaceous plots undergoing different fertilization treatments. Vertical bars represent standard errors.